e-J. Surf. Sci. Nanotech. Vol. 10 (2012) 310-314 Conference - ISSS-6 -

Atomic and Electronic Structures of Si(111)-$\sqrt{21} \times \sqrt{21}$ Superstructure*

Y. Fukaya†
Advanced Science Research Center, Japan Atomic Energy Agency, 1233 Watanuki, Takasaki, Gunma 370-1292, Japan

K. Kubo, T. Hirahara, and S. Yamazaki
Department of Physics, University of Tokyo, 7-3-1 Hongo, Bunkyo-ku, Tokyo 113-0033, Japan

W. H. Choi and H. W. Yeom
Department of Physics and Center for Atomic Wires and Layers, Pohang University of Science and Technology, Pohang 790-784, Korea

A. Kawasuso
Advanced Science Research Center, Japan Atomic Energy Agency, 1233 Watanuki, Takasaki, Gunma 370-1292, Japan.

S. Hasegawa
Department of Physics, University of Tokyo, 7-3-1 Hongo, Bunkyo-ku, Tokyo 113-0033, Japan.

I. Matsuda‡
ISSP, University of Tokyo, 5-1-5, Kashiwanoha, Kashiwa, Chiba 277-8581, Japan
(Received 31 January 2012; Accepted 29 May 2012; Published 7 July 2012)

The $\sqrt{21} \times \sqrt{21}$-(Au,Ag) phase on a Si(111) surface, prepared by the Ag deposition on the Si(111)-5 × 2-Au surface, was studied by using angle-resolved photoemission spectroscopy (ARPES) and scanning tunneling microscopy (STM). The surface phase is metallic and has a two-dimensional electronic structure similar to those of the $\sqrt{21} \times \sqrt{21}$ phases prepared by noble metal adsorption on the Si(111)-$\sqrt{3} \times \sqrt{3}$-Ag surface. An additional surface-state was found, which may originate from the Au 6*s* and 6*p* orbitals. [DOI: 10.1380/ejssnt.2012.310]

Keywords: Two-dimensional alloys; Silicon; Gold; Silver; Electronic structure; Surface structure; Angle-resolved photoemission spectroscopy (ARPES); Scanning tunneling microscopy (STM)

I. INTRODUCTION

Noble metal adsorption on a silicon crystal surface has been a prototype system of metal/semiconductor interfaces. By depositing one monolayer (ML) of Ag atoms on a Si(111)-7 × 7 surface at around 740 K, the Si(111)-$\sqrt{3} \times \sqrt{3}$-Ag surfaces are formed. Here, the coverage (ρ) of 1 ML is defined as 7.83×10^{14} cm^{-2}. To date, the Si(111)-$\sqrt{3} \times \sqrt{3}$-Ag surfaces have been extensively investigated as a typical two-dimensional metal system [1, 2]. Additional adsorptions of small amounts of noble and alkali metal atoms on the Si(111)-$\sqrt{3} \times \sqrt{3}$-Ag surfaces lead to the formation of $\sqrt{21} \times \sqrt{21}$ superstructures with a dramatic increase in the surface electrical conductivity [1, 2]. The atomic coordinates of the $\sqrt{21} \times \sqrt{21}$ superstructures have been studied both experimentally and theoretically [3–12]. In the cases of noble metal adsorptions, we found that three noble atoms in the unit cell are situated at the centers of large Ag triangles, surrounding the Si timer [9, 10] (see Fig. 1). According to the scanning tunneling microscopy (STM) observations [13], the alkali metal induced $\sqrt{21} \times \sqrt{21}$ superstructure is considered to be different from the noble metal induced ones. The electronic structures for the Si(111)-$\sqrt{21} \times \sqrt{21}$-Ag and Si(111)-$\sqrt{21} \times \sqrt{21}$-(Ag,Au) surfaces have been also extensively investigated [14–19]. The previous angle-resolved photoemission spectroscopy (ARPES) studies indicate a similarity in electronic structures for the Si(111)-$\sqrt{21} \times \sqrt{21}$-Ag and Si(111)-$\sqrt{21} \times \sqrt{21}$-(Ag,Au) surfaces. Recently, we found that the $\sqrt{21} \times \sqrt{21}$ superstructure is also formed by the additional deposition of the Ag atoms onto the Si(111)-5 × 2-Au ($\rho_{\mathrm{Au}} = 0.40$ ML) and Si(111)-$\sqrt{3} \times \sqrt{3}$-Au ($\rho_{\mathrm{Au}} = 0.90$ ML) surfaces [20]. This result indicates that when the total coverage of the noble metals corresponds to approximately 1.14 ML, the $\sqrt{21} \times \sqrt{21}$ superstructures appear on the Si(111) surface. Thus, from the metallurgical point of view, $\sqrt{21} \times \sqrt{21}$ superstructures have attracted much attention as two-dimensional electron compound alloys [20–24]. In previous studies [25], using the reflection high-energy positron diffraction, we investigated the atomic structures of the Si(111)-$\sqrt{21} \times \sqrt{21}$-(Au,Ag) surface, where the Si(111)-5 × 2-Au surface is used as the substrate. We showed that the atomic structure of the Si(111)-$\sqrt{21} \times \sqrt{21}$-(Au,Ag) surface is very similar to those with different stoichiometries of Ag and Au atoms [25]. In this study, in order to understand the $\sqrt{21} \times \sqrt{21}$ superstructures comprehensively, we investigated the atomic and electronic structures of the Si(111)-$\sqrt{21} \times \sqrt{21}$-(Au,Ag) surface using the ARPES and STM. We demonstrate that the ARPES spectra and STM images for the Si(111)-$\sqrt{21} \times \sqrt{21}$-

*This paper was presented at the 6th International Symposium on Surface Science –Towards Nano, Bio and Green Innovation–, Tower Hall Funabori, Tokyo, Japan, December 11-15, 2011.
†Corresponding author: fukaya.yuki99@jaea.go.jp
‡Corresponding author: imatsuda@issp.u-tokyo.ac.jp

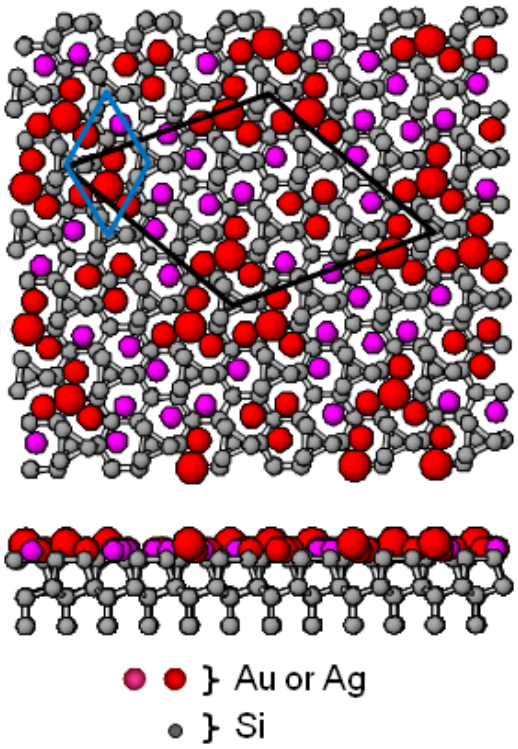

FIG. 1: Schematic drawings of structure model of the Si(111)-$\sqrt{21}\times\sqrt{21}$ superstructure. Large circles denote the adatoms of the Ag or Au atoms. Medium and small circles show the Ag or Au and Si atoms, respectively. Unit cells of the $\sqrt{21}\times\sqrt{21}$ and $\sqrt{3}\times\sqrt{3}$ are indicated by the black and blue lines, respectively.

(Au,Ag) surface show a similarity in electronic states for the Si(111)-$\sqrt{21}\times\sqrt{21}$ surfaces with different stoichiometries of Au and Ag atoms.

II. EXPERIMENTAL

The substrates were cut from a mirror-polished Si(111) wafer. To prepare clean 7×7 surfaces, they were flashed at 1470 K in a few seconds several times in an ultra-high vacuum (UHV) chamber. Then, 0.40 ± 0.08 ML of the Au atoms were deposited on the Si(111)-7×7 surfaces at 870 K to form the 5×2-Au structures. Finally, 0.74 ± 0.10 ML of the Ag atoms were deposited on the Si(111)-5×2-Au surfaces at 720 K. The deposition rates of the Au and Ag atoms were calibrated from the formations of the β-$\sqrt{3}\times\sqrt{3}$-Au and the $\sqrt{3}\times\sqrt{3}$-Ag structures on the Si(111) surfaces. The well-ordered Si(111)-$\sqrt{21}\times\sqrt{21}$-(Au,Ag) surfaces were characterized by reflection high-energy electron diffraction. Electronic bands were measured by the ARPES instrument with unpolarized He Iα radiation. Core-level spectra were recorded with linearly polarized synchrotron radiation on beamline BL-8A1 at Pohang Light Source in Korea. The STM images were taken at room temperature using a commercial STM system (UNISOKU USM-501). The details of experiments were described elsewhere [8, 17].

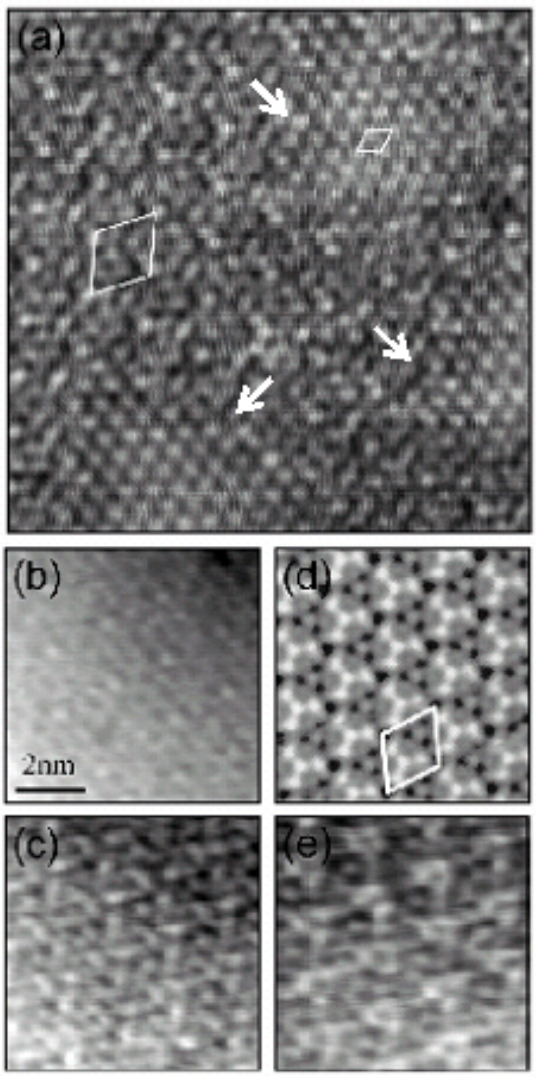

FIG. 2: (a) Filled-state (tip bias voltage (V_t) +2.0 V) STM current image of the Si(111)-$\sqrt{21}\times\sqrt{21}$-(Au,Ag) surface at room temperature. Large and small rhombuses indicate unit cells of $\sqrt{21}\times\sqrt{21}$ and $\sqrt{3}\times\sqrt{3}$, respectively. The $\sqrt{3}\times\sqrt{3}$ domains in the $\sqrt{21}\times\sqrt{21}$ phase are indicated by the white arrows. Enlarged (b) filled- ($V_t=+1.0$ V) and empty-state ((c) $V_t=-1.0$ V and (e) $V_t=-1.5$ V) topographic images of the Si(111)-$\sqrt{21}\times\sqrt{21}$-(Au,Ag) surface at room temperature. For comparison, filled-state ($V_t=+1.5$ V) topographic image of the Si(111)-$\sqrt{21}\times\sqrt{21}$ surface, where the Ag atoms of 0.14 ML are deposited on the Si(111)-$\sqrt{3}\times\sqrt{3}$-Ag surface, is also displayed in (d) [14]. The rhombus in (d) shows the $\sqrt{21}\times\sqrt{21}$ unit cell.

III. RESULTS AND DISCUSSION

Figure 2(a) shows the filled-state STM image of the Si(111)-$\sqrt{21}\times\sqrt{21}$-(Au,Ag) surface taken at room temperature. In the STM images, well-ordered $\sqrt{21}\times\sqrt{21}$ domains are visible in wide areas. In some parts, the small $\sqrt{3}\times\sqrt{3}$ domains are observed, as indicated by small rhombus in Fig. 2(a). This result indicates that the underlying structure of the $\sqrt{21}\times\sqrt{21}$ domains is composed of the $\sqrt{3}\times\sqrt{3}$ structure. It is noted that the bright protrusions in the $\sqrt{3}\times\sqrt{3}$ domain (denoted as arrows in Fig. 2(a)) resemble to those of the inequiva-

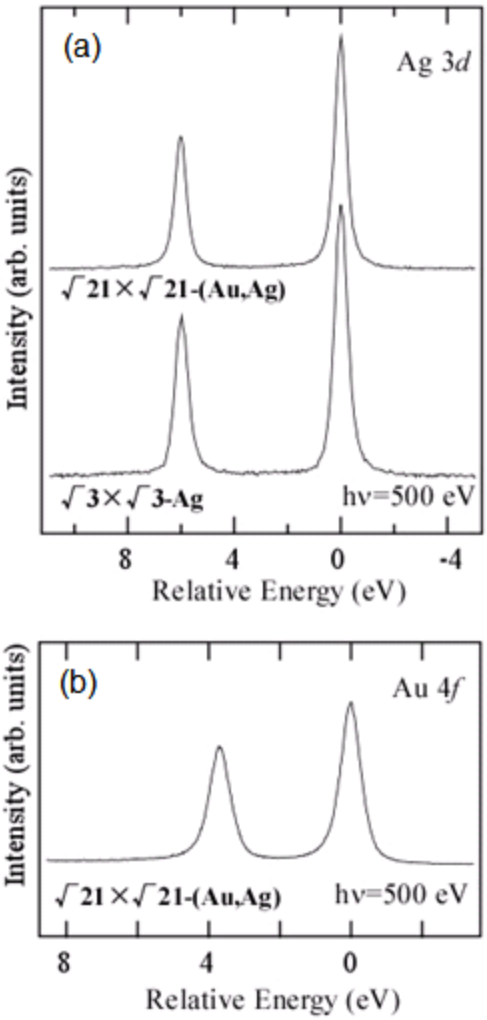

FIG. 3: (a) Ag 3*d* core-level photoemission spectra of the Si(111)-$\sqrt{21}\times\sqrt{21}$-(Au,Ag) and Si(111)-$\sqrt{3}\times\sqrt{3}$-Ag surfaces. (b) Au 4*f* core-level spectrum of the Si(111)-$\sqrt{21}\times\sqrt{21}$-(Au,Ag) surface [25].

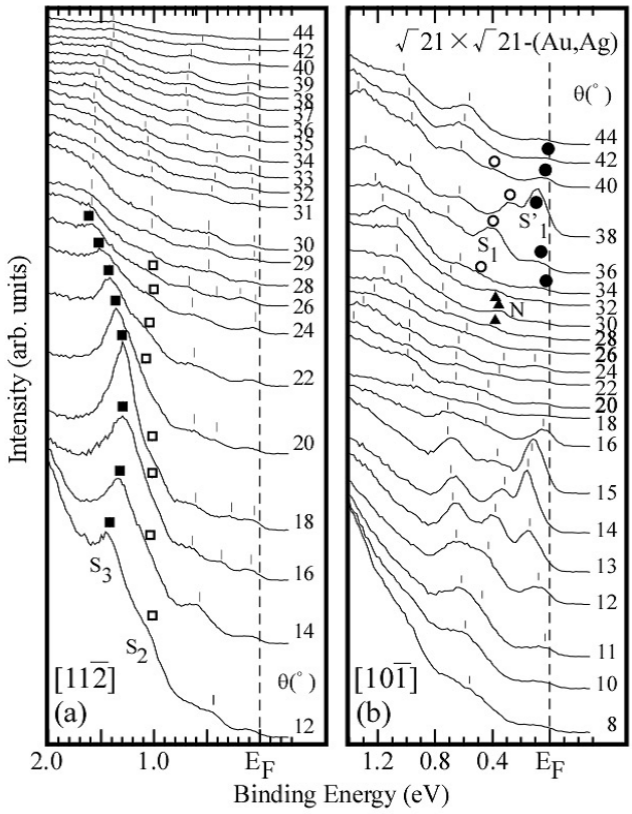

FIG. 4: Angle-resolved photoemission spectra of the Si(111)-$\sqrt{21}\times\sqrt{21}$-(Au,Ag) surface as a function of emission angle (θ) along (a) the [11$\bar{2}$] and (b) [10$\bar{1}$] directions.

lent triangle (IET) structure of the Si(111)-$\sqrt{3}\times\sqrt{3}$-Ag surface at low temperature [26]. Since the amount of the deposited Ag atoms is lower than 1 ML, the coverage required to make the IET structure of the Si(111)-$\sqrt{3}\times\sqrt{3}$-Ag surface, the IET structure cannot be constructed only by the Ag atoms. In the Si(111)-$\sqrt{21}\times\sqrt{21}$-(Au,Ag) surface, therefore, the alloys including both Ag and Au atoms construct the IET structure. This result infers that the IET structure composed of the Ag-Au alloys is kept up to room temperature in contrast to the Si(111)-$\sqrt{3}\times\sqrt{3}$-Ag surface, where the IET structure fluctuates above 130 K.

Figure 2(b) and 2(c,e) display the filled- and empty-state STM images of the Si(111)-$\sqrt{21}\times\sqrt{21}$-(Au,Ag) surface at room temperature, respectively. As shown in the empty-state images of Figs. 2(c) and 2(e), the protrusions in the $\sqrt{21}\times\sqrt{21}$ domains are similar to those of the $\sqrt{21}\times\sqrt{21}$ structures with $\rho_{\rm Ag}$ = 1.14 ML and $\rho_{\rm Au}$ = 0.00 ML [5] and $\rho_{\rm Ag}$ = 1.00 ML and $\rho_{\rm Au}$ = 0.14 ML [3, 4, 8]. Therefore, the adatom configurations of the Si(111)-$\sqrt{21}\times\sqrt{21}$-(Au,Ag) surface are expected to be similar to the two other $\sqrt{21}\times\sqrt{21}$ surfaces with different stoichiometries of Au and Ag atoms.

On the other hand, we notice that the filled-state image of Fig. 2(b) is slightly different from those of the other $\sqrt{21}\times\sqrt{21}$ structure with different stoichiometries of Au and Ag atoms [Fig. 2(d)]. Although bright propeller-like protrusions are clearly visible in the other $\sqrt{21}\times\sqrt{21}$ structure with different stoichiometries [8, 14], these protrusions on the Si(111)-$\sqrt{21}\times\sqrt{21}$-(Au,Ag) surface are blurred and only the centers of them are distinct. This might originate from the Au atoms embedded into the $\sqrt{3}\times\sqrt{3}$ structure. As shown in the following section, a new state below Fermi level, together with the electronic band structure of the $\sqrt{3}\times\sqrt{3}$ structure is observed in the ARPES spectra. The difference of the filled-state images between the $\sqrt{21}\times\sqrt{21}$ structures with different stoichiometries may be explained by the existence of the new state.

In order to investigate the chemical environments of the Ag and Au atoms, we measured the core-level photoemission spectra from the Si(111)-$\sqrt{21}\times\sqrt{21}$-(Au,Ag) surface. Figure 3(a) shows the Ag 3*d* core-level spectra of the Si(111)-$\sqrt{21}\times\sqrt{21}$-(Au,Ag) and Si(111)-$\sqrt{3}\times\sqrt{3}$-Ag surfaces. The Ag 3*d* spectra of both surfaces are almost the same and can be fitted by a single Voigt function with a spin-orbit splitting [25]. The result indicates that the chemical environment of Ag atoms in the Si(111)-$\sqrt{21}\times\sqrt{21}$-(Au,Ag) surface is very close to that in the Si(111)-$\sqrt{3}\times\sqrt{3}$-Ag surface. Figure 3(b) shows the Au 4*f* core-level spectrum of the Si(111)-$\sqrt{21}\times\sqrt{21}$-(Au,Ag) surface. The Au 4*f* spectrum is also fitted by a single

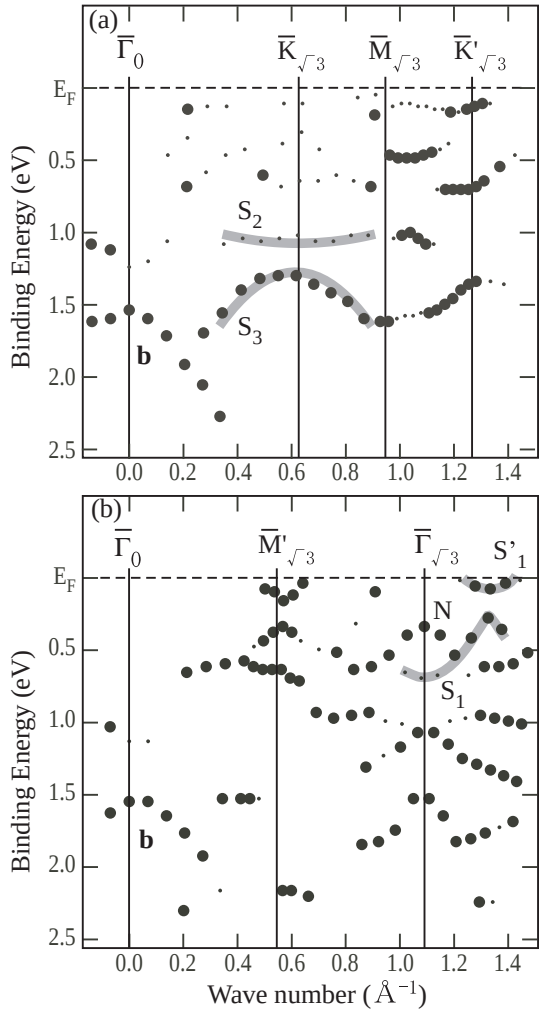

FIG. 5: Electronic band structures constructed by the angle-resolved photoemission spectra (Fig. 4) from the Si(111)-$\sqrt{21} \times \sqrt{21}$-(Au,Ag) surface along (a) the [11$\bar{2}$] and (b) [10$\bar{1}$] directions. The *b* state indicates the bulk Si one.

Voigt function with a spin-orbit splitting. Thus, the Au atoms in the Si(111)-$\sqrt{21} \times \sqrt{21}$-(Au,Ag) phase have the same chemical environment. These findings indicate that the Ag and Au atoms are homogeneously distributed in the Si(111)-$\sqrt{21} \times \sqrt{21}$-(Au,Ag) phase and occupy the specific sites in the unit cells. Therefore, the Si(111)-$\sqrt{21} \times \sqrt{21}$-(Au,Ag) surface is considered to be a regular alloy phase.

Figures 4(a) and 4(b) represent the ARPES spectra measured from the Si(111)-$\sqrt{21} \times \sqrt{21}$-(Au,Ag) surface along the [11$\bar{2}$] and [10$\bar{1}$] directions, respectively. In Fig. 4(a), we found that the binding energy of the S_2 state is almost constant against the change of the photoemission angle (θ) while the S_3 state disperses drastically. In Fig. 4(b), we can identify a few surface states in the spectra. In the θ range of $30^\circ - 40^\circ$, in particular, three surface states denoted as S_1, S'_1, and N appear near the Fermi level E_F with characteristic dispersions.

Figures 5(a) and 5(b) represent the electronic band structures of the Si(111)-$\sqrt{21} \times \sqrt{21}$-(Au,Ag) surface along the [11$\bar{2}$] and [10$\bar{1}$] directions, respectively. In Fig. 5(a), two bands assigned as S_2 and S_3 for the Si(111)-$\sqrt{3} \times \sqrt{3}$-Ag surface are observed [27]. From the STM observations, this band structure supports the formation of the IET structure in the Si(111)-$\sqrt{21} \times \sqrt{21}$-(Au,Ag) surface. In Fig. 5(b), the S_1 band appears only at $\bar{\Gamma}$ point and disperses toward E_F. The new band denoted as N appears near $\bar{\Gamma}$ point and is characteristic of the Si(111)-$\sqrt{21} \times \sqrt{21}$-(Au,Ag) surface. The N band may originate from $6s$ and $6p$ orbitals of Au atoms in the $\sqrt{3} \times \sqrt{3}$ structure. The slight difference of the filled-state STM images between the Si(111)-$\sqrt{21} \times \sqrt{21}$-(Au,Ag) surface and the other Si(111)-$\sqrt{21} \times \sqrt{21}$ surfaces with different stoichiometries of Au and Ag atoms is considered to originate from the existence of the new N band (see Fig. 2(b)). Therefore, the electronic band structures are consistent with the STM images observed.

The S_1 band in the Si(111)-$\sqrt{3} \times \sqrt{3}$-Ag surface shifts to the higher binding energy due to the electron doping from the adatoms on the IET structure in the Si(111)-$\sqrt{21} \times \sqrt{21}$-(Au,Ag) surface. Then, the Fermi circle crosses the zone boundary of the Si(111)-$\sqrt{21} \times \sqrt{21}$-(Au,Ag) surface. Consequently, the S_1 band folds back at the zone boundary and splits into two states denoted as S_1 and S'_1 with an energy gap of $\sim$0.15 eV. The Fermi wave vector of the S'_1 band is estimated to $\sim$0.24 Å^{-1}. The value is very close to that for the Si(111)-$\sqrt{21} \times \sqrt{21}$ surface with different stoichiometries of Au and Ag atoms [17, 28]. This mechanism of the band folding is consistent with the previous studies on the Si(111)-$\sqrt{21} \times \sqrt{21}$-Ag and Si(111)-$\sqrt{21} \times \sqrt{21}$-(Ag,Au) surfaces [17, 28]. As a result, the electronic band structure of the Si(111)-$\sqrt{21} \times \sqrt{21}$-(Au,Ag) surface is very close to those of the other Si(111)-$\sqrt{21} \times \sqrt{21}$ surfaces with different stoichiometries, except for the new (N) state.

IV. CONCLUSION

With regards to stoichiometries of Au and Ag atoms, the Si(111)-$\sqrt{21} \times \sqrt{21}$-(Au,Ag) surface is different from the Si(111)-$\sqrt{21} \times \sqrt{21}$-Ag and Si(111)-$\sqrt{21} \times \sqrt{21}$-(Ag,Au) surfaces. Irrespective of the different stoichiometries of Au and Ag atoms, the underlying structure for the Si(111)-$\sqrt{21} \times \sqrt{21}$-(Au,Ag) surface is composed of the IET structure, which is observed for the Si(111)-$\sqrt{3} \times \sqrt{3}$-Ag surface. Furthermore, the electronic structure of the Si(111)-$\sqrt{21} \times \sqrt{21}$-(Au,Ag) surface is also similar to the two other Si(111)-$\sqrt{21} \times \sqrt{21}$ surfaces with different stoichiometries of Au and Ag atoms.

Acknowledgments

WHC and HWY are supported by CRi program of MEST, Korea. The present work was partly supported by Grant-in-Aid for Young Scientists (B) 22740205 from JSPS.

[1] S. Hasegawa, X. Tong, S. Takeda, N. Sato, and T. Nagao, Prog. Surf. Sci. **60**, 89 (1999).
[2] S. Hasegawa, J. Phys.: Condens. Matter **12**, R463 (2000).
[3] J. Nogami, K. J. Wan, and X. F. Lin, Surf. Sci. **306**, 81 (1994).
[4] A. Ichimiya, H. Nomura, Y. Horio, T. Sato, T. Sueyoshi, and M. Iwatsuki, Surf. Rev. Lett. **1**, 1 (1994).
[5] X. Tong, Y. Sugiura, T. Nagao, T. Takami, S. Takeda, S. Ino, and S. Hasegawa, Surf. Sci. **408**, 146 (1998).
[6] H. Aizawa and M. Tsukada, Phys. Rev. B **59**, 10923 (1999).
[7] H. Tajiri, K. Sumitani, W. Yashiro, S. Nakatani, T. Takahashi, K. Akimoto, H. Sugiyama, X. Zhang, and H. Kawata, Surf. Sci. **493**, 214 (2001).
[8] C. Liu, I. Matsuda, M. D'angelo, S. Hasegawa, J. Okabayashi, S. Toyoda, and M. Oshima, Phys. Rev. B **74**, 235420 (2006).
[9] Y. Fukaya, A. Kawasuso, and A. Ichimiya, Surf. Sci. **600**, 3141 (2006).
[10] Y. Fukaya, A. Kawasuso, and A. Ichimiya, Surf. Sci. **601**, 5187 (2007).
[11] H. Jeong, H. W. Yeom, and S. Jeong, Phys. Rev. B **76**, 085423 (2007).
[12] X. Xie, J. M. Li, W. G. Chen, F. Wang, S. F. Li, Q. Sun, and Y. Jia, J. Phys.: Condens. Matter **22**, 085001 (2010).
[13] C. Liu, I. Matsuda, H. Morikawa, H. Okino, T. Okuda, T. Kinoshita, and S. Hasegawa, Jpn. J. Appl. Phys. **42**, 1659 (2003).
[14] X. Tong, S. Ohuchi, N. Sato, T. Tanikawa, T. Nagao, I. Matsuda, Y. Aoyagi, and S. Hasegawa, Phys. Rev. B **64**, 205316 (2001).
[15] H. M. Zhang, K. Sakamoto, and R. I. G. Uhrberg, Phys. Rev. B **64**, 245421 (2001).
[16] H. M. Zhang, K. Sakamoto, and R. I. G. Uhrberg, Phys. Rev. B **70**, 245301 (2004).
[17] I. Matsuda, T. Hirahara, M. Konishi, C. Liu, H. Morikawa, M. D'angelo, and S. Hasegawa, Phys. Rev. B **71**, 235315 (2005).
[18] M. Konishi, I. Matsuda, C. Liu, H. Morikawa, and S. Hasegawa, e-J. Surf. Sci. Nanotech. **3**, 107 (2005).
[19] C. Liu, I. Matsuda, T. Hirahara, S. Hasegawa, J. Okabayashi, S. Toyoda, and M. Oshima, Surf. Sci. **602**, 3316 (2008).
[20] I. Matsuda, F. Nakamura, K. Kubo, T. Hirahara, S. Yamazaki, W. H. Choi, H. W. Yeom, H. Narita, Y. Fukaya, M. Hashimoto, A. Kawasuso, M. Ono, Y. Hasegawa, S. Hasegawa, and K. Kobayashi, Phys. Rev. B **82**, 165330 (2010).
[21] W. Hume-Rothery, R. E. Smallman, and C. W. Haworth, *The Structure of Metals and Alloys* (The Metals and Metalurgy Trust, London, 1969).
[22] T. B. Massalski and U. Mizutani, Prog. Mater. Sci. **22**, 151 (1978).
[23] G. Trambly de Laissardiere, D. Nguyen-Manh, and D. Mayou, Prog. Mater. Sci. **50**, 679 (2005).
[24] Y. Fukaya, I. Matsuda, M. Hashimoto, H. Narita, A. Kawasuso, and A. Ichimiya, e-J. Surf. Sci. Nanotech. **7**, 432 (2009).
[25] Y. Fukaya, I. Matsuda, M. Hashimoto, K. Kubo, T. Hirahara, S. Yamazaki, W. H. Choi, H. W. Yeom, S. Hasegawa, A. Kawasuso, and A. Ichimiya, Surf. Sci. **606**, 919 (2012).
[26] H. Aizawa, M. Tsukada, N. Sato, and S. Hasegawa, Surf. Sci. **429**, L509 (1999).
[27] I. Matsuda, H. Morikawa, C. Liu, S. Ohuchi, S. Hasegawa, T. Okuda, T. Kinoshita, C. Ottaviani, A. Cricenti, M. D'angelo, P. Soukiassian, and G. Le Lay, Phys. Rev. B **68**, 085407 (2003).
[28] J. N. Crain, K. N. Altmann, C. Bromberger, and F. J. Himpsel, Phys. Rev. B **66**, 205302 (2002).